ANTIBODY TO H+ V-ATPase SUBUNIT E COLOCALIZES WITH PORTASOMES IN ALKALINE LARVAL MIDGUT OF A FRESHWATER MOSQUITO (*AEDES AEGYPTI* L.)

ZHENGPENG ZHUANG, PAUL J. LINSER AND WILLIAM R. HARVEY*

The Whitney Laboratory, University of Florida, 9505 Ocean Shore Boulevard, St Augustine, FL 32086, USA

*Author for correspondence (e-mail: wharvey@whitney.ufl.edu)

Summary

The pH profile, gross structure, ultrastructure and immunolabeling of the mosquito (*Aedes aegypti*) larval midgut are described as a first step in analyzing the role of plasma membrane H+ V-ATPase in the alkalization of the gut, nutrient uptake and ionic regulation. Binding of an antibody to H+ V-ATPase subunit E colocalizes with 'portasomes' (approximately 10 nm in diameter), which are thought to correspond to the V_1 part of the H+ V-ATPase. In gastric caeca (pH 8), both antibody-binding sites and portasomes are located apically; in the anterior midgut (pH 10–11), they are located basally; and in the posterior midgut (pH≈8) they are again located apically. The hypothesis that the energization of alkalization is mediated by an H+ V-ATPase is supported by the inability of larvae to maintain the high pH after 72 h in 10 μM bafilomycin B1. Confirming earlier reports, the two principal epithelial cell types are designated as 'columnar' and 'cuboidal' cells. The apical plasma membranes (microvilli) of epithelial cells in the gastric caeca and basal infoldings of anterior midgut are invaded by mitochondria that lie within approximately 20 nm of the portasome-studded plasma membranes.

The colocalization of V-ATPase-immunolabeling sites and portasomes to specific plasma membranes within so-called 'mitochondria-rich' cells of gastric caeca and anterior midgut suggests that midgut alkalization in mosquitoes is achieved by molecular mechanisms similar to those that have been described in caterpillars, even though the gross structure of the midgut and the localization of the V-ATPase are dissimilar in the two species. In caterpillars, the high alkalinity is thought to break down dietary tannins, which block nutrient absorption; it may play a similar role in plant-detritus-feeding mosquito larvae. The colocalization of immunolabeling sites and portasomes, together with the presence of long, 'absorptive-type' microvilli in the posterior midgut, suggest that the V-ATPase energizes nutrient uptake there.

Key words: gastric caecum, subunit E, bafilomycin, mosquito, *Aedes aegypti*, H+ V-ATPase, portasome, midgut.

Introduction

The pH can exceed 12 in the midgut of caterpillars and mosquito larvae (Dow, 1984). The alkalinity is thought to aid in the breakdown of dietary tannins, which interfere with nutrient absorption (Berenbaum, 1980). The alkalization mechanism is partially understood in caterpillars, especially in the model lepidopteran insect *Manduca sexta*, in which a proton pump (H+ V-ATPase; Schweikl et al., 1989; Wieczorek et al., 1986, 1989, 1990) hyperpolarizes the apical membranes of specialized 'goblet cells' (Harvey et al., 1983) to 240 mV (Dow and Peacock, 1989). The voltage drives an electrophoretic exchange (antiport) of luminal H+ for cellular K+, which accounts, in part, for the alkalinity of the lumen (Wieczorek et al., 1991; Azuma et al., 1995; for a review see Wieczorek et al., 1999). The voltage also appears across the adjacent columnar cell apical membrane (brush-border membrane), where it drives electrophoretic cotransport (symport) of amino acids, coupled to K+, from the

lumen into the cells (Harvey and Wieczorek, 1997; Castagna et al., 1998; D. H. Feldman, W. R. Harvey and B. R. Stevens, manuscript in preparation).

Little is known about the alkalization mechanism in mosquito larvae beyond the observations of Dadd (1975, 1976) that the pH can exceed 11 in anterior midgut (e.g. in *Aedes aegypti*), but is lower in posterior midgut (pH 8), and that it is rapidly but reversibly lowered by agents or conditions that interfere with cellular respiration. The ultrastructure of the larval midgut of fresh water mosquito has been studied (Volkmann and Peters, 1989a,b) but not in relation to solute transport (Cioffi, 1984). Are 'goblet cells' present in mosquito larval midgut and do they play a role in alkalization? Do an H+ V-ATPase and H+-coupled antiporter energize the alkalization, and, if so, which plasma membranes are energized? To begin answering such questions we have

analyzed the structure and ultrastructure of the midgut of larval *Aedes aegypti* and localized the H$^+$ V-ATPase by immunohistochemistry. Our results are consistent with the hypothesis that an H$^+$ V-ATPase does energize the alkalization of mosquito larval midgut and that the process may be similar at the plasma membrane level to that in caterpillars, even though the tissue and cellular structures are quite different in the two types of insect.

Materials and methods

Rearing mosquitoes

Dry *Aedes aegypti* L. eggs were provided by Dr D. R. Barnard of the Center for Medical, Agricultural and Veterinary Entomology, Gainesville, Florida, USA. Eggs (approximately 0.4 ml total volume) were placed in a glass bottle (30 ml, half-filled with aerated well water) along with 1–2 drops of artificial food consisting of 30 g of bovine liver powder and 20 g of baker's yeast in 1 l of water. After vigorously agitating the eggs and food in the bottle, the mixture was allowed to stand for 2 h while the larvae hatched. The hatchlings were transferred to a plastic tray (50×25×10 cm) which was half-filled with well water and 30–50 ml of the artificial food. Trays were kept in a cool (25 °C) dimly lit room until the fourth instar larvae were removed for study.

Preparation and fixation of tissue

To dissect out the midgut, the anal segment together with the saddle papillae and head were removed using forceps, and the remaining body was gently teased apart, starting with the thorax, where the gastric caeca are located. In some cases, the gut contents enclosed in the peritrophic membrane simply slid out, leaving behind the empty midgut, which was pulled out using forceps. The isolated midguts from approximately 20 individuals were placed in ice-cold, freshly prepared 3 % glutaraldehyde overnight at 4 °C. The tissue was rinsed seven times in 0.1 mol l^{-1} sodium phosphate buffer, pH 7.2, then placed in 1 % osmium tetroxide, in the same buffer, for 1 h at 4 °C. Samples were subsequently rinsed twice with ice-cold distilled water and dehydrated in an ethanol series (50 %, 75 %, once each for 15 min; 95 %, 100 % twice each for 15 min), culminating in two changes of propylene oxide with a waiting period of 15 min after each change. The samples were then placed in Epon mixture/propylene oxide (1/1) for 45 min at room temperature (22–25 °C). Finally, samples were transferred from vials into fresh Epon mixture in molds and polymerized in an oven at 60 °C for 72 h.

Light and electron microscopy

Semithin (0.5–1.5 μm) sections were cut with a diamond knife (Micro Star) on a Sorvall Porter-Blum ultramicrotome (MT-2) and stained with 1 % Methylene Blue for approximately 4 min at 94 °C. The Methylene Blue solution was freshly prepared, by mixing equal volumes of 1 % Methylene Blue plus 1 % sodium citrate together with 1 % Azure II, and filtered prior to being mixed for staining.

Ultrathin (7–12 nm) sections (i.e. silver to gold) were cut with the same knife. The sections were collected on grids and stained with 3 % aqueous uranyl acetate for 8 min followed by staining for 16 min in lead citrate (Reynolds, 1963). Sections were examined with a JEM-100 CXII transmission electron microscope opeating at 60 kV.

Immunocytochemistry

Using the methods of Linser et al. (1997), larvae were fixed overnight in 4 % paraformaldehyde and then cryoprotected in 30 % sucrose in Tris-buffered saline (TBS). They were then embedded in OCT compound (Tissue-Tek) and stored at −30 °C until they solidified. Frozen sections (10–12 μm) were cut and incubated with primary monoclonal antibody (hybridoma supernatant) against H$^+$ V-ATPase for 1 h. Antibody binding was visualized using fluorescein isothiocyanate (FITC)-conjugated secondary antibody at a dilution recommended by the commercial producer (goat anti-mouse IgG; Jackson Immuno Research Laboratories Inc). The same sections were counterstained with 4′,6-diamidino-2-phenylindol (DAPI) to visualize cell nuclei (Linser et al., 1997) and Rhodamine-conjugated Phalloidin (Sigma) to visualize muscles.

pH measurements in vivo

Early fourth instar larvae (5–6 days after hatching) were removed from the rearing tray and placed in an activated charcoal suspension in aerated well water for 12–24 h. Appropriate pH-sensitive dyes (see below) were mixed with kaolin at 1:100 (w/w) and 100 mg of the kaolin/dye mixture was suspended in 0.5 ml of 100 % ethanol. The dye/kaolin/ethanol mixture was then diluted 1:100 with well water. Groups of approximately 50 larvae were then placed in a Petri dish (8 cm diameter) containing 50 ml of the final dye-labeled kaolin mixture. After 24–36 h, larvae were viewed at 10–40× magnification from their ventral side with a Nikon (SMZ-10) dissecting microscope. To estimate its pH, each body segment was compared visually with a series of pH-sensitive dye standards, with pH values ranging from 4–11. The standards were prepared in steps of approximately 0.5 pH units by placing dye-kaolin mixtures in a 5 ml glass vial with 5–6 volumes of an appropriate 0.2 mol l^{-1} pH buffer solution. The dyes were: Thymol Blue (red, pH≤1.2; dark yellow, pH≥2.8; light yellow, pH≤8.0; white, pH 8.0; blue/purple, pH≥9.2), m-Cresol Purple (red, pH≤1.2; yellow, pH≥2.8; dark yellow, pH≤7.4; purple, pH≥9.0), Phenol Red (yellow, pH≤6.8; red, pH≥8.2) and Thymolphthalein (blue, pH≥10.1).

The effects of bafilomycin B1 on the larval luminal pH were observed using pH-sensitive dyes (Dadd, 1975). For each trial, 50 fourth-instar larvae were placed in a Petri dish (8 cm diameter, 1.5 cm deep) with 50 ml of well water and a 1:100 dye:kaolin mixture. A stock solution of bafilomycin B1 (10 mmol l^{-1}; Fluka) was prepared in ethanol, and appropriate amounts were added to achieve the desired final concentrations. Controls were prepared by adding ethanol alone to the well water.

Results

The midgut of *Aedes aegypti* fourth instar larvae (approximately 3 mm long and 0.4 mm diameter) is divided into four parts (Fig. 1A,B); from anterior to posterior they are as follows: cardia (not shown), gastric caeca, anterior midgut and posterior midgut. The demarcation between midgut and hindgut is just anterior to the junction of the Malpighian tubules and gut. For brevity, only structures related to transport are described, although other structures are identified in the figure legends.

pH profile, bafilomycin

The overall pH profile in the midgut of a larva that had ingested Thymol Blue is shown in a low-magnification, ventral image of *Aedes aegypti* fourth instar larvae (Fig. 1C): the gastric caeca are mildly alkaline (yellow, pH≤8.0) the anterior midgut is highly alkaline (blue, pH≥9.2) and the posterior midgut, mildly alkaline (white, pH≈8.0). Thymolphthalein, which exhibits color gradations at higher pH than Thymol Blue, confirmed Dadd's (1975) report that the gut pH exceeded 10 (not shown).

The pH of gastric caeca and anterior midgut in fourth instar mosquito larvae is normally ≥9.2, and these parts appear red when Phenol Red is added. However, after exposure for 72 h to 10 μmol l^{-1} bafilomycin B1, the majority of the larvae had a pH≤9.2 in three separate experiments (Table 1).

Light microscopy of epithelium

The midgut epithelium consists of a single layer of cells with an apical brush border and an uneven basal border (Fig. 2). The brush border protrudes into the ectoperitrophic space, which is separated from the midgut contents by the peritrophic membrane. The basal margin of the cells is striated and is bounded by a basal lamina that is surrounded periodically by circular muscles which, in turn, are surrounded by longitudinal muscles. Tracheal trunks penetrate these layers, branch extensively, and terminate in end cells (not shown) that exchange oxygen and carbon dioxide directly with the epithelial cells. The large size of the cells, often >50 μm tall, their arrangement in a one-cell-thick epithelium in which apical, lateral and basal plasma membrane sectors are readily identifiable, and the ease of isolating the intact midgut, all facilitate the localization of membrane transport proteins within the epithelium.

Gastric caeca

A cross section of this region shows six of the eight outpockets of the epithelium which form cavities that connect medially with the midgut lumen (Fig. 3A). Dark- and light-staining cells are designated columnar cells and cuboidal cells, respectively. An extensive brush border is also evident (Fig. 3A). A band of dark-staining inclusion bodies is located immediately subjacent to the apical microvilli of the brush border. The basal side of the epithelial cells is lightly stained, which reflects labyrinthine infoldings of the plasma membrane that frequently penetrate the cell even to the level of the nucleus.
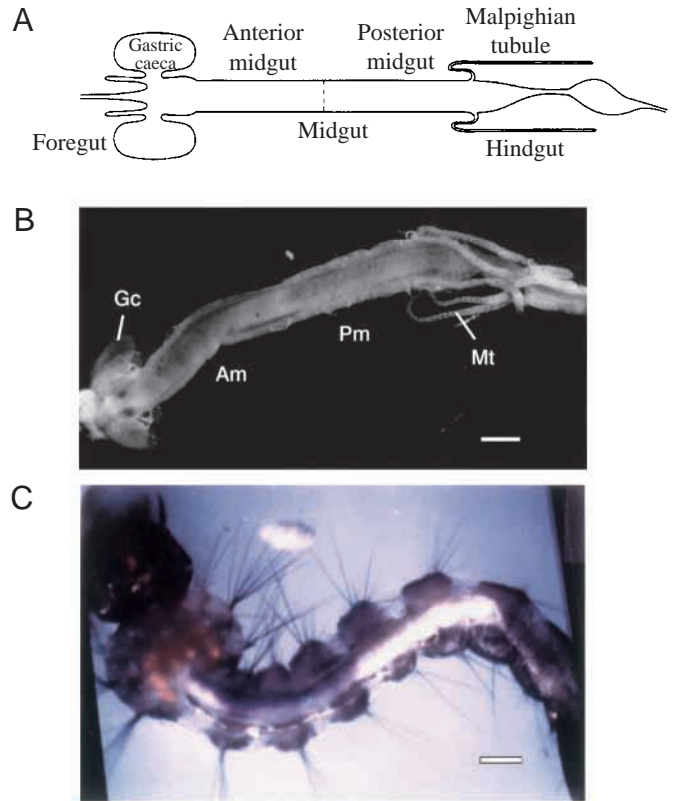

Fig. 1. (A) Diagram of the mosquito midgut. (B) Light micrograph of the *Aedes aegypti* fourth instar larvae midgut. After the anteriormost gastric caeca (Gc), the midgut narrows and then broadens to a tube-like 'anterior midgut' (Am), followed by the 'posterior midgut' (Pm). The midgut ends at the point where it is joined by Malpighian tubules (Mt). Scale bar, 0.5 mm. (C) Low-magnification image of living fourth instar *Aedes aegypti* larva, showing a mildly alkaline pH in the gastric caeca, a highly alkaline pH in the anterior midgut (body segments 1–3) and a mildly alkaline pH in the posterior midgut (body segments 4–8). Thymol Blue is blue/purple in color when the pH is above 9.2. Scale bar, 0.5 mm.

Anterior midgut region

Just posterior to the gastric caeca the midgut first narrows and then widens to a straight tube (approximately 0.5 mm diameter), the anterior midgut (Fig. 1B), which can be distinguished from the posterior midgut by its relatively smaller cells (Fig. 2). The anterior midgut epithelium is a simple cylindrical wall approximately 45 μm thick that

Table 1. *Number of* Aedes aegypti *fourth instar larvae with midgut pH >9.2 after exposure to bafilomycin B1 for 72 h*

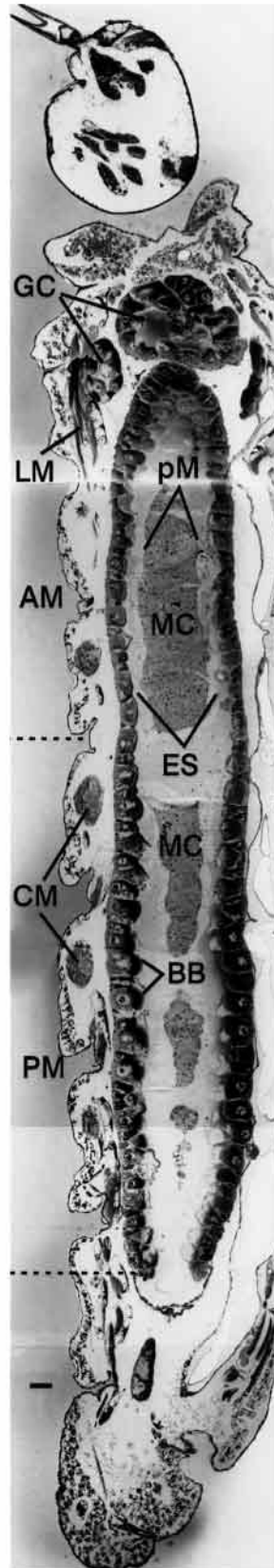| Trial	N	Bafilomycin B1 concentration (μmol l^{-1})	
		0	10
1	50	48	10
2	50	49	2
3	50	48	1

Fig. 2. Longitudinal section of a fourth instar *Aedes aegypti* larva showing general anatomy of the alimentary canal at low magnification. GC, gastric caeca; AM, anterior region of midgut; PM, posterior region of midgut between dashed lines; MC, midgut contents; pM, peritrophic membrane; ES, ectoperitrophic space; BB, brush border; CM, circular muscles; LM, longitudinal muscle. Scale bar, 50 μm.
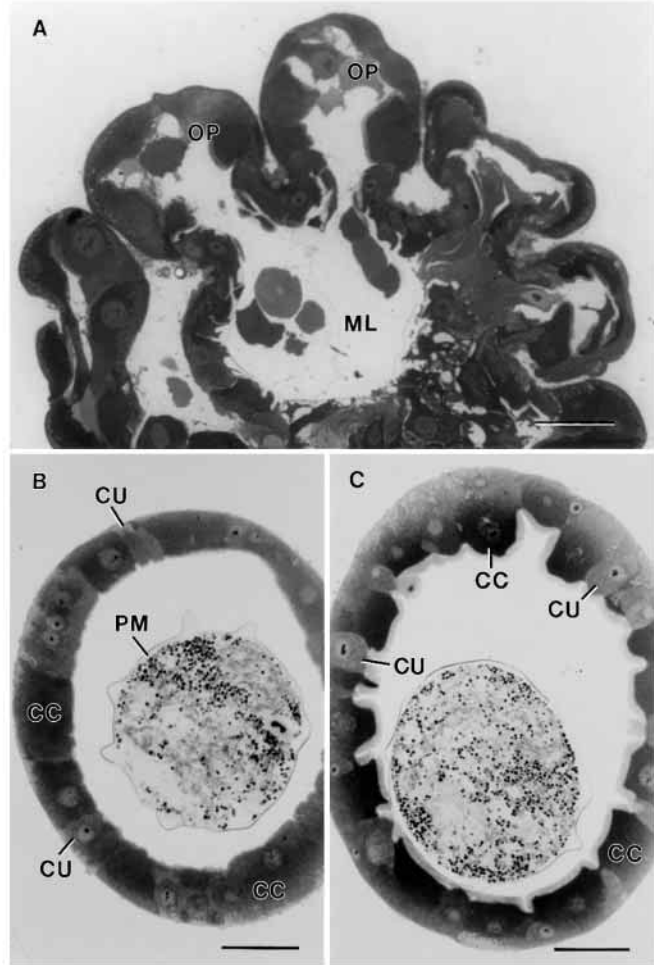

Fig. 3. Transverse sections of the gastric caeca (A), the anterior midgut (B) and the posterior midgut (C). In A, gastric caeca columnar epithelial cells bound the OP (outpockets) of the ML (midgut lumen). CU, cuboidal cells; CC, columnar cells; PM, peritrophic membrane. Scale bars, 20 μm.

(Fig. 3B). Food particles in the lumen are enclosed in a thin peritrophic membrane. Both the large columnar cells (approximately 45 μm tall and 30 μm wide) and the less frequent cuboidal cells have large, central nuclei (approxiamtely 15 μm diameter). There is no apical brush border and the luminal margin is smooth (Fig. 3B).

Posterior midgut

A cross section of posterior midgut (Fig. 3C) shows darkly staining columnar cells, lightly stained cuboidal cells and occasional, basally located regenerative cells (not shown). The apical brush border is 5–7 μm long on these tall columnar cells, which extend further into the lumen than the cuboidal cells, rendering the luminal margin uneven.

Electron microscopy of major cells

The epithelium of larval *Aedes aegypti* midgut contains numerous mitochondria-rich cells (Brown and Breton, 1996) in which particle-studded plasma membranes lie uniformly

contains approximately 35 cells in a typical cross section, and encloses a lumen of approximately 350 μm in diameter
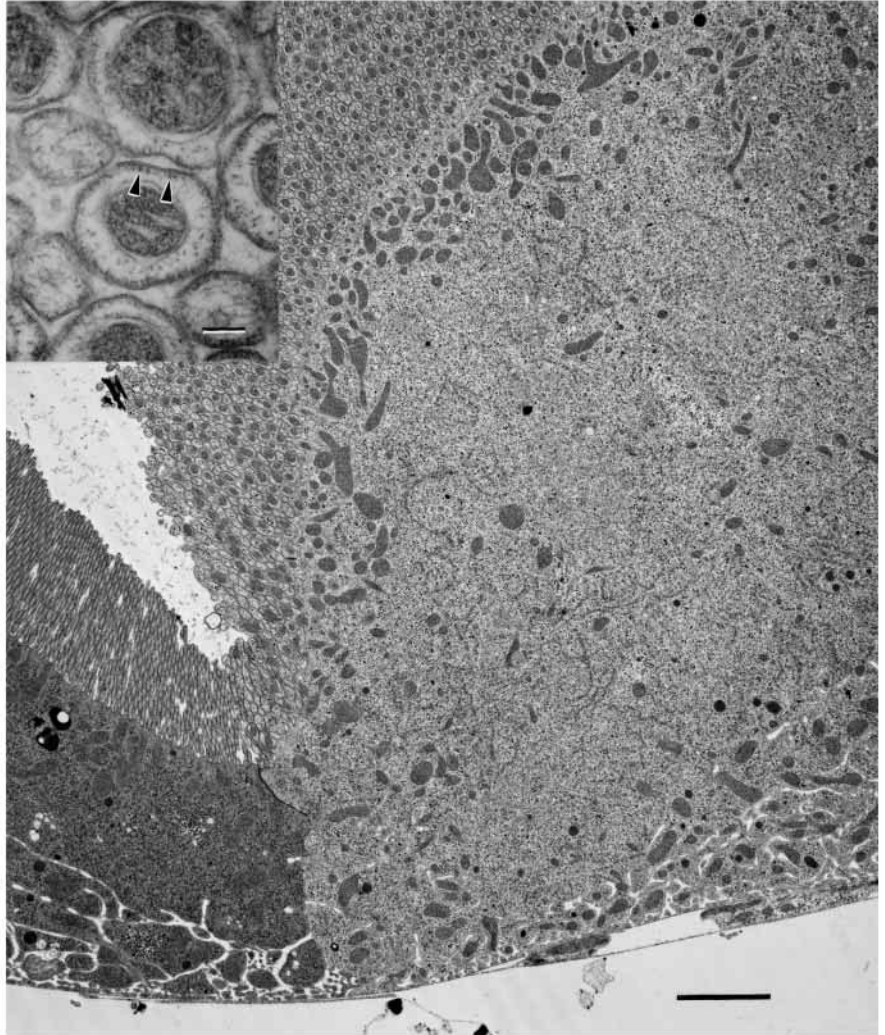
Fig. 4. Gastric caeca: electron micrograph of two epithelial cells. The lightly staining 'ion-transporting cell' (on the right) has microvilli (shown in cross section) containing mitochondria. The darker staining of the resorptive or secretory cell (left), is due to the presence of extensive rough endoplasmic reticulum. Scale bar, 5 μm. The inset is a high-magnification electron micrograph of a transverse section from an ion-transporting cell (such as the cell on the right) with microvilli that contain mitochondria. Portasomes (arrowheads) are prominent on the cytoplasmic face of the membrane. Scale bar, 100 nm.

close to mitochondria. The particles are approximately 10 nm in diameter and, occasionally, can be seen to rest on a stalk approximately 10 nm in length. The epithelium also contains numerous cells in which mitochondria are numerous but are not closely associated with particle-studded membranes. There appears to be no correspondence between the columnar and cuboidal cells seen in the light micrographs and the mitochondria-rich, particle-studded cells and the other cells. It is possible that cuboidal cells are merely a stage in the development of columnar cells.

Gastric caeca

Electron micrographs from the gastric caeca of larval *Aedes aegypti* (Fig. 4) resemble those from larval *Culex pipiens* (Volkmann and Peters, 1989a,b) and earlier electron micrographs (Jones and Zeve, 1968) in that two types of cell are visible. In one cell type (Fig. 4, left) there are long, thin microvilli that do not contain mitochondria, and the cytoplasm is very electron-dense. The other cell type has long, thick, microvilli, each of which contains a mitochondrion. Moreover, there are numerous elongated mitochondria at the base of the microvilli and partially within them (Figs 4, 5). The cell shown

in Fig. 5 is strongly reminiscent of those from salt-water mosquito larvae in which mitochondria have been reported to move into and out of microvilli in response to osmotic stress (Bradley and Satir, 1981). At higher magnification, a cross section of the mitochondria-containing microvilli reveals that the plasma membranes are studded on their cytoplasmic surface with particles that are approximately 10 nm in dimeter (Fig. 4, inset); the particles are even more prominent on the cytoplasmic surface when the mitochondria-filled microvilli are shown in longitudinal section (Fig. 5, inset), where it is clear that the particles are no more than 20 nm from the mitochondria in many places.

Anterior midgut

Extensive infoldings of the basal plasma membrane penetrate almost half-way into the cells, forming parallel cisternae (Fig. 6A). Numerous mitochondria are closely associated with these basal membrane infoldings, which are studded with particles approximately 10 nm across (Fig. 6C, courtesy of Moria Cioffi). The apical microvilli are very short (approximately 1 μm long and 0.4 μm wide) (Fig. 6B). A tracheal cell is visible just outside the basal lamella (Fig. 6D).
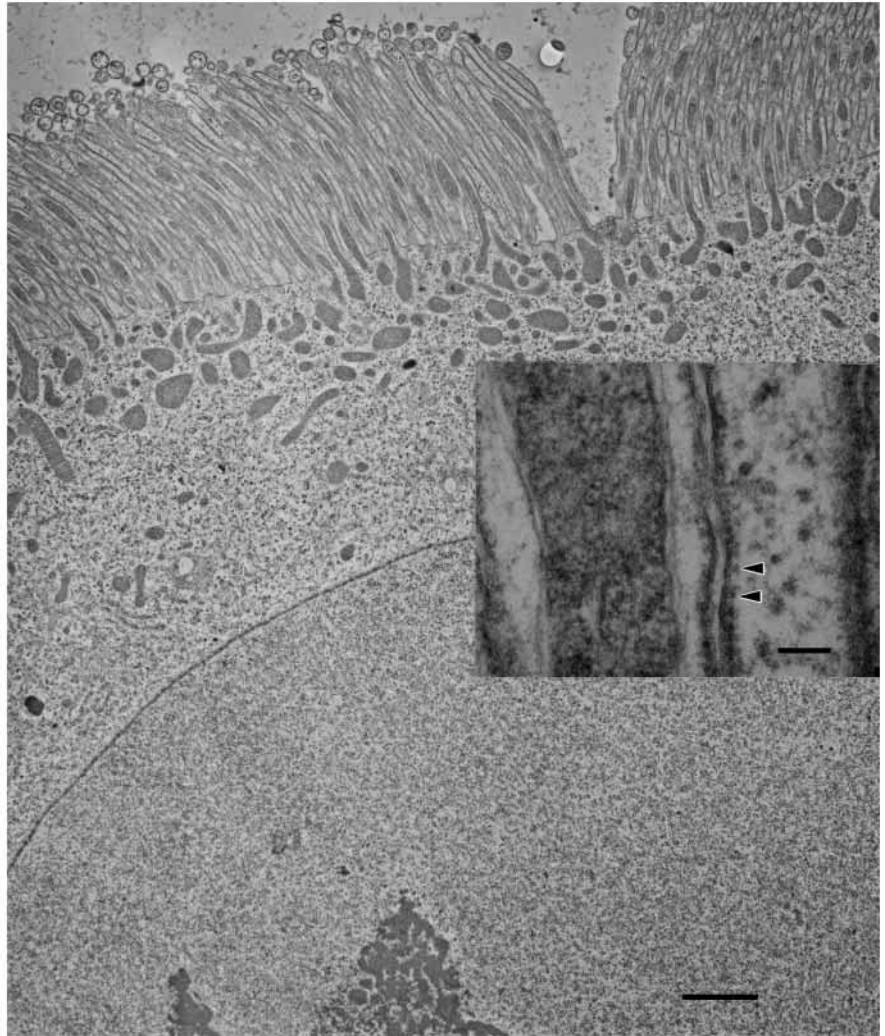
Fig. 5. Gastric caeca: electron micrograph of an epithelial cell. 'Stretched' mitochondria that have partially or totally invaded the microvilli are seen in the apical portion of this ion-transporting cell. Scale bar, 2 μm. The inset is a high-magnification, longitudinal view of mitochondria within microvilli. Portasomes (arrowheads) are visible on the cytoplasmic side of the microvillar membrane. Scale bar, 100 nm.

Posterior midgut

The posterior midgut cells (Fig. 7) have numerous, long, thin, apical microvilli (>10 μm long, 0.2 μm wide; Fig. 7, inset). Each microvillus is a distinct structure with no connection to adjacent microvilli and no branches along its entire length. Mitochondria are abundant in both the apical and basal regions of the posterior midgut cells. However, the apical mitochondria do not invade the microvilli which, nevertheless, appear to be heavily studded on their cytoplasmic surface with particles approximately 10 nm in diameter (Fig. 7, inset): the particles are not well-defined, perhaps because of the 'fuzzy' glycocalyx that is present on the outer side of the microvilli.

Electron microscopy of minor cells

Regenerative cells

These undifferentiated 'stem' cells (Hecker, 1977) are found in all three parts of the midgut. They are invariably located at the base of the epithelium and are normally enclosed between two columnar cells. They are so small (approximately 7 μm in diameter) that they are barely visible with the light microscope. Regenerative cells are characterized by a nucleus that occupies most of the volume of the cell and a scant cytoplasm that contains small amounts of both rough and smooth endoplasmic reticulum along with a few mitochondria (not shown).

Tracheal cells

Tracheal cells are always found on the haemolymph side of the basement membrane. The cell shown in Fig. 6D is oval in shape with a wave-like, highly electron-dense circle of chitinous cuticle along the luminal edge.

Endocrine cells

Aedes aegypti larval midguts presumably also contain endocrine cells, like those found in adults (Brown et al., 1985), but none was identified positively in this study.

Failure to detect goblet cells

From the longitudinal sections and cross sections, we estimate that the midgut contains at least 3000 columnar and/or cuboidal cells, but no apparent goblet cells. Our observations, along with numerous older studies of larval mosquito cytoarchitecture, make it very clear that these mosquito larvae do not possess any cell type with the unique structural characteristics of the goblet cells of the larval lepidopteran midgut.
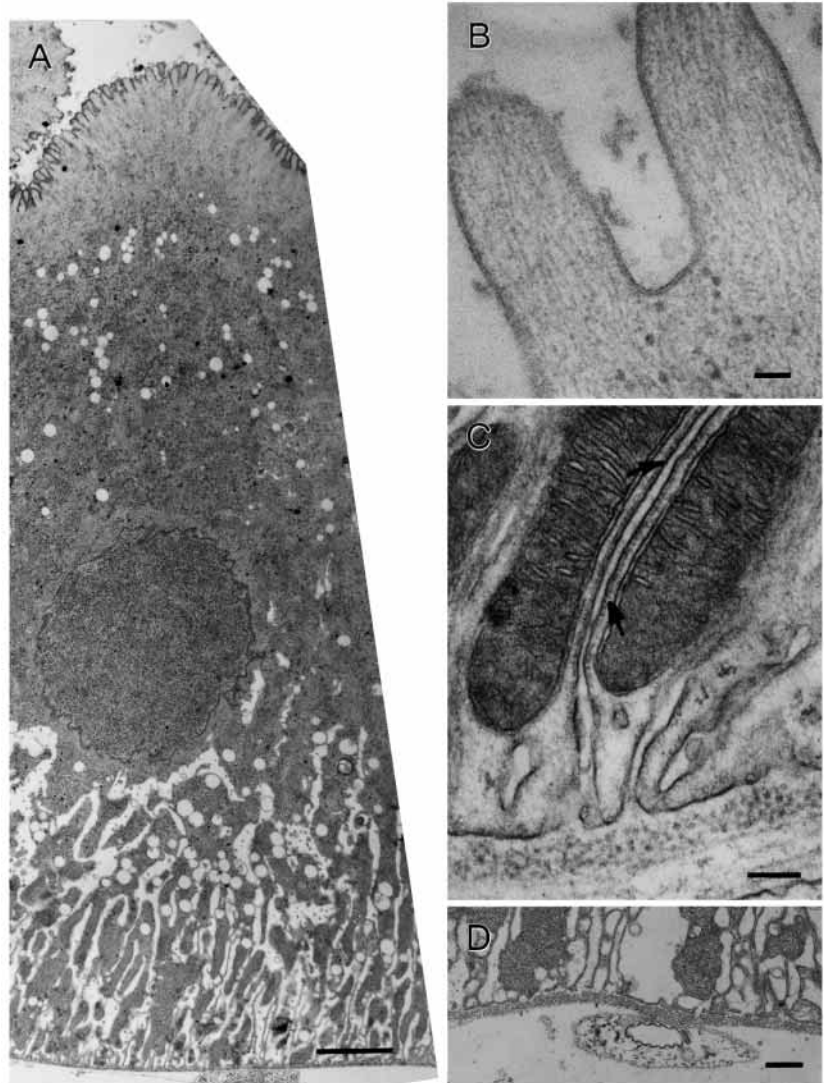
Fig. 6. Anterior midgut: electron micrographs of epithelial cell. (A) This cross section shows short, broad, apical microvilli (top). Subjacent to the microvilli is a zone of lighter electron density. Infoldings of the basal plasma membranes extend to the nucleus and are closely associated with mitochondria. Scale bar, 7 μm. (B) A high-magnification micrograph of the apical portion of the cell, showing two short microvilli without visible portasomes. Scale bar, 100 nm. (C) A high-magnification micrograph of the basal portion of the cell. Portasomes (arrows) stud the cytoplasmic side of the infolding basal membranes. Scale bar, 100 nm. (D) A low-magnification micrograph of a tracheal cell on the haemolymph side of the basement membrane. Scale bar, 10 μm.

Immunofluorescence labeling of Aedes aegypti larval midgut

Frozen sections 10–12 μm thick were probed with a monoclonal antibody (mAb184-3) specific for *Manduca sexta* midgut H^+ V-ATPase (U. Klein, personal communication). This antibody has been used by several investigators to localize plasma membrane H^+ V-ATPase in a number of insects (e.g. Garayoa et al., 1995; Just and Walz, 1994). The antibody was used to localize the V-ATPase in sections of larval midgut. Because of the resistance of the chitin exoskeleton of the larvae to cryosectioning, isolated gut preparations produced the best structural analyses of mAb184-3 immunolocalization. Guts were sectioned both longitudinally and in cross section. Sections were counter-labeled with DAPI and Rhodamine-conjugated Phalloidin to visualize the nuclei and muscles (actin), respectively. Fig. 8 shows representative results of our findings. Strong V-ATPase immunofluorescence labeling (yellow/green) was found in the apical region of most epithelial cells in the gastric caeca (Fig. 8A,D) and the apical region of many epithelial cells in posterior midgut (Fig. 8C,F). In contrast, the labeling was observed in the basal region of the epithelial cells in anterior midgut (Fig. 8B,E). The mesh of radial and longitudinal muscle fibers that surrounds the gut tube (red, Phalloidin staining) serves as a clear marker of the hemolymph side of the epithelium (Fig. 8). Our results show that the localization of mAb184-3 labeling, and thus the presence of plasma membrane H^+ V-ATPase, changes from apical membranes (gastric caeca) to basal membranes (anterior midgut) to apical membranes (posterior midgut) along the course of this continuous epithelial tube. Controls using either non-relevant primary antibodies or the complete omission of primary antibody demonstrated the staining patterns to be specific to the mAb184-3 (not shown).

Discussion

V-ATPases energize larval Aedes aegypti midgut plasma membranes

The hypothesis that alkalizing plasma membranes of mosquito larval midguts are energized by H^+ V-ATPases, is supported by five lines of evidence: (i) all eukaryotic cells
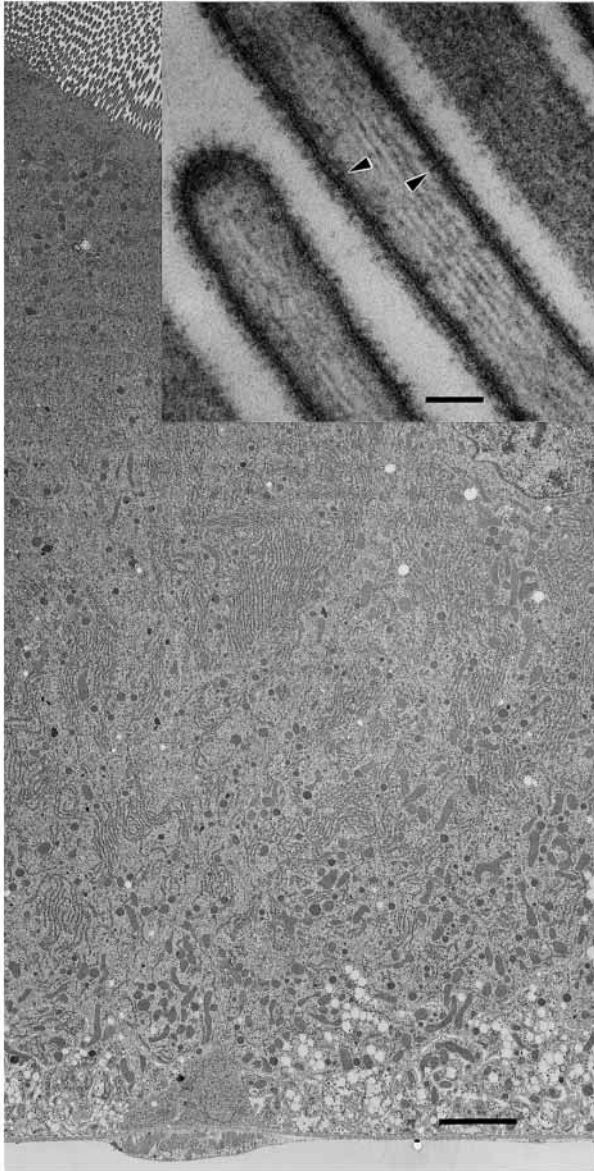
Fig. 7. Posterior midgut: low-magnification electron micrograph of an epithelial cell. Extensive, long, thin microvilli appear wave-like rather than perfectly straight. A section cannot therefore go longitudinally through the entire length of all microvilli, resulting in a large amount of circular-to-oval profiles found on the luminal side. 'Stack' and simple 'whorl' rough endoplasmic reticulum is visible in the cytoplasm. Mitochondria are located on both the apical and basal sides of the cell. Scale bar, 5 μm. The inset is a high-magnification view of the apical microvilli showing a 'fuzzy' glycocalax coat on its outer side. Putative portasomes (arrowheads) are seen on the cytoplasmic side of the membrane. Scale bar, 100 nm.

express V-ATPases; (ii) larval midgut alkalization is inhibited by bafilomycin; (iii) antibody to V-ATPase subunit E immunolabels the apical region of gastric caeca, the basal region of anterior midgut and the apical region of posterior midgut; (iv) portasomes colocalize with the immunolabeling; and (v) the immunolabeled, portasome-studded membranes are hyperpolarized.

All eukaryotic cells have V-ATPases

The ubiquitous distribution of V-ATPases in endomembranes of all eukaryotic cells is well known (for reviews see Stevens and Forgac, 1997; Nelson and Harvey, 1999). V-ATPase subunits A and c have been cloned from *Aedes aegypti* larval midgut (Gill et al., 1998). How are the plasma membranes that are responsible for alkalization of larval mosquito midgut energized by V-ATPases?

Aedes aegypti *midgut alkalization is inhibited by bafilomycin*

Phenol Red color changes indicate that the pH, which is normally >8 in gastric caeca and >10.5 in anterior midgut, falls to <8 in both regions after prolonged exposure to 10 μM bafilomycin (Table 1 and unpublished observations). The pH drops much more quickly following inhibition of cellular respiration by lack of oxygen, cooling or chloroform (Dadd, 1976) than it does in response to bafilomycin. The delay in response to bafilomycin probably reflects the time required for this hydrophobic molecule to reach its intramembrane binding site, which may be on the approx. 100 kDa subunit (for a review, see Dröse and Altendorf, 1997). The cryptic binding site and partitioning of bafilomycin into other membrane lipids probably account for the micromolar concentrations required to inhibit V-ATPase *in vivo* compared with the nanomolar concentrations that suffice to inhibit the purified enzyme. Similar high concentrations of bafilomycin are required to inhibit V-ATPase-mediated processes in frog skin (Klein et al., 1997) and caterpillar (*Manduca sexta*) midgut (Schirmanns and Zeiske, 1994).

Antibody to V-ATPase labels specific plasma membranes

Immunolabeling with antibody to V-ATPase (mAb184-3) was restricted to the apical regions of gastric caeca (Fig. 8A,D), basal regions of anterior midgut (Fig. 8B,E) and apical regions of posterior midgut (Fig. 8C,F). In each case, the broad area of labeling corresponds approximately to the area occupied by microvilli or basal infoldings of respective plasma membranes, as defined by the electron microscopy.

mAb184-3 is a monoclonal antibody that was generated against highly purified V-ATPase holoenzyme from *M. sexta* larval midgut (U. Klein, personal communication). This antibody has been used to identify V-ATPase in many tissues, including the salivary glands of cockroaches (*Periplaneta americana*) (Just and Walz, 1994), the Malpighian tubules of ants (*Formica polyctena*) (Garayoa et al., 1995), the salivary glands of *Aedes aegypti* (M. G. Novak and J. Ribeiro, personal communication) and the hindgut of the locust (*Schistocerca gregalia*) (U. Klein, personal communication) as well as the goblet cells of larval *Manduca sexta*. The antibody should be useful in the future to affinity-purify V-ATPase protein from *Aedes Aegypti* larvae, facilitating further characterization of the mosquito enzyme.

Portasomes colocalize with immunolabeling

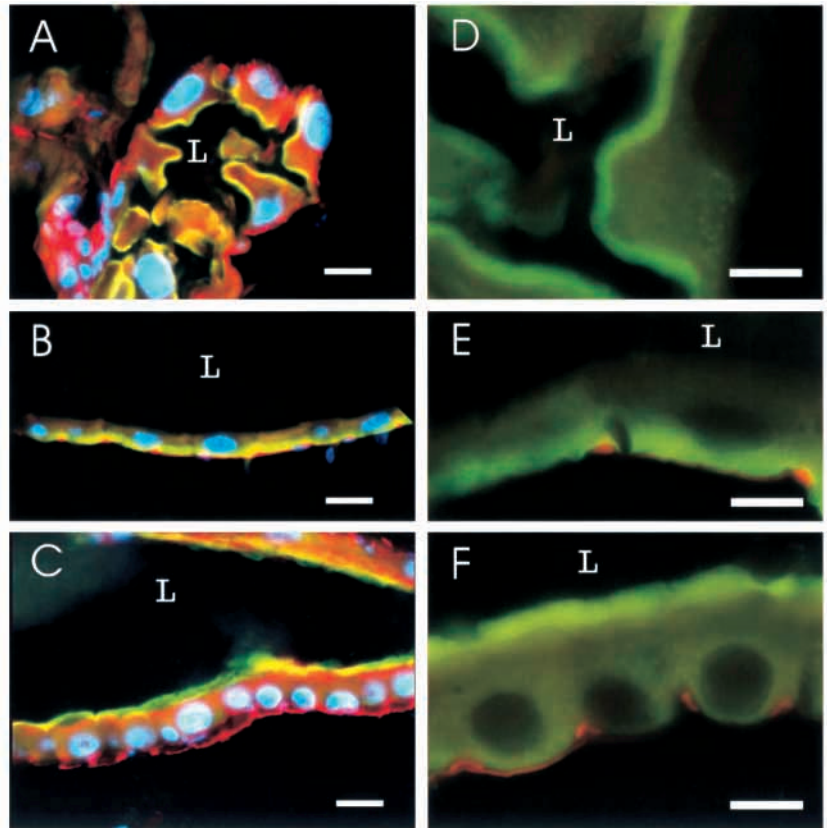In numerous cases where electrophysiology and histochemistry have identified plasma membranes that are

Fig. 8. Immunolocalization of V-ATPase using monclonal antibody 184-3 (yellow/green) contrasted with DAPI labeling of nuclei (blue) and Phalloidin labeling of muscles (red) (A–C). Higher magnifications are shown monochromatically (FITC, green) with slight red bleed-through (D–F). The V-ATPase antibody specifically labeled the apical side (facing the lumen, L) of most epithelial cells in the gastric caeca (A,D); it labeled the basal side (away from the lumen) of cells in anterior midgut (B,E), and it labeled the apical side of cells in posterior midgut (C,F). The basket of longitudinal and radial muscles that surrounds the full extent of the midgut is demonstrated by the periodic rhodamine (red) staining of the basal side of the epithelium. Scale bars, 20 µm.

energized by H+ V-ATPases, their cytoplasmic faces have been studded with stalked particles approximately 10 nm in length (Gupta and Berridge, 1966; Anderson and Harvey, 1966) known as 'portasomes' (i.e. transport bodies; for a review, see Harvey, 1992). Portasomes were used as markers to isolate pure goblet cell apical membranes (Cioffi and Wolfersberger, 1983; Harvey et al., 1983) from which midgut V-ATPase was subsequently solubilized (Schweikl et al., 1989). In a few cases, biochemical and immunohistochemical studies have confirmed that portasomes are V_1 sectors of the V-ATPase (e.g. Gräf et al., 1996). Most recently, six dense areas (presumably the three A and three B subunits) surrounding a central dense area have been visualized directly in electron micrographs of isolated portasomes (Rademacher et al., 1999), showing that portasomes do indeed correspond to V_1 particles.

Particles are present on specific plasma membranes in all three midgut regions. The particles are spheres approximately 10 nm in diameter and are connected by roughly 10 nm long stalks to the membranes. The pattern of distribution of these particles observed in the electron micrographs corresponds exactly to the pattern of labeling by the antibody to V-ATPase. Thus, the particles on the apical plasma membrane colocalize with apical immunofluorescence in gastric caeca (compare Fig. 8A with insets of Figs 4, 5). The particles on the basal plasma membrane colocalize with basal immunofluorescence in the anterior midgut (compare Figs 8B, 6C). Finally, the particles on the apical plasma membrane colocalize with apical immunofluorescence in the posterior midgut (compare

Figs 8C, Fig. 7 inset). Moreover, the particle density on each of the three plasma membrane sectors is high enough to account for the observed immunolabeling. Endomembranes, in which ATPase particle density is lower, are not characteristically visualized by antibodies to V-ATPase subunits. Clearly, the particles studding the mosquito membranes are portasomes, implying that they are V_1 ATPase sectors.

The immunolabeled, portasome-studded membranes are hyperpolarized

The basal plasma membrane in anterior midgut and the apical plasma membrane in posterior midgut are hyperpolarized (Clark et al., 1999). These are precisely the membrane sectors that are immunolabeled with the V-ATPase mAb184-3 and are portasome-studded. Hyperpolarization of these membrane sectors is to be expected, since V-ATPases always extrude protons from cells and are electrogenic. Clark et al. (1999) did not study the gastric caeca but, on the basis of immunolabeling and portasome-studding, one can predict that their apical membranes will be hyperpolarized in this midgut region.

Consistency of evidence for plasma membrane V-ATPase in mosquito larvae

Taken separately, the arguments for V-ATPase energization of mosquito larval midgut have some shortcomings. The immunolabeling by antibody to V-ATPase might be an artifact

due to an epitope shared between this enzyme and a different protein. The particles on specific membranes might be other large proteins that happen to be of the same size and shape as portasomes. The hyperpolarizations reported by Clark et al. (1999) decay with time and require 5-hydroxytryptamine to be restored. However, taken together, the arguments are convincing. It is highly unlikely that, in three midgut regions, labeling and particles would colocalize by chance and that in two of the regions hyperpolarization would colocalize as well.

Alkalinity and midgut function

The region in mosquito larval midgut that most resembles the caterpillar midgut is the gastric caeca. Not only are the apical membranes immunolabeled and portasome-studded, but the eight caecal chambers in mosquito midguts may be the functional equivalent of the goblet cavities of caterpillar midguts. In that case, the mildly alkaline pH in gastric caeca is puzzling, since the machinery for extreme alkalization would appear to be present. Perhaps alkali secreted by the gastric caeca is titrated by tannic acid from ingested plant detritus. When the titration is complete, the pH could rise to values near 11 in the next section, i.e. the anterior midgut, where tannins could be broken down. Then, in posterior midgut, where tannins would now be absent, nutrient absorption could proceed in the mildly alkaline environment (Fig. 1C). However, the larva of Fig. 1C was fed on a yeast diet, which is low in tannins, and then starved by feeding kaolin, and yet the gastric caecal pH remained mildly alkaline. Another possibility was suggested by Volkmann and Peters (1989b), who proposed that fluid flows from posterior midgut to gastric caeca in the ectoperitrophic space, increasing caecal [K$^+$] while rendering caecal pH mildly alkaline. This seems unlikely because the peritrophic membrane (in caterpillars) is freely permeable to small solutes (Gringorten et al., 1993).

Lumen alkalization by basally localized V-ATPase

Maximal alkalization takes place in anterior midgut, where ATPase is located basally. This unexpected finding demonstrates that an apical localization is not necessary for alkalization of the lumen. Upon reflection, a basal localization would be expected intuitively for lumen alkalization, because a basal ATPase would pump protons out of cells and away from the lumen; a basal localization of V-ATPase is well known in B cells of rat kidney (Brown et al., 1992). By contrast lumen alkalinization by the apically located V-ATPase in caterpillar (*Manduca sexta*) midgut goblet cells is counterintuitive; protons are pumped towards the lumen, hyperpolarizing the apical membrane to −240 mV, which drives K$^+$ to the lumen *via* an apical, electrophoretic K$^+$/2H$^+$ antiporter (Wieczorek et al., 1991; Azuma et al., 1995) and/or an apical amino-acid-gated, OH$^-$ channel (D. H. Feldman, W. R. Harvey and B. R. Stevens, in preparation).

V-ATPase energization of nutrient uptake in posterior midgut

The V-ATPase is localized apically in posterior midgut by immunolabeling, portasome-studding and hyperpolarization, but the apical membrane is not associated with mitochondria (Fig. 9 inset). The apical microvilli are long and of the absorptive type (Cioffi, 1979). The simplest hypothesis is that the V-ATPase hyperpolarizes the apical membrane and that K$^+$ is cotransported with amino acids, from lumen to cell. The presence of absorptive microvilli in posterior midgut is consistent with Wigglesworth's (1942) observation that, after *Aedes aegypti* larvae had been fed glucose or starch and casein, the posterior midgut was a major site for absorption and storage of glycogen. By contrast, the short, broad microvilli of the anterior midgut are not adapted for nutrient uptake, and the mitochondria-filled microvilli in certain gastric caecal cells are better-adapted for K$^+$ secretion than for amino acid absorption.

Goblet cells are not necessary for alkalization

Alkalization in mosquito larvae occurs in the absence of goblet cells. In contrast to caterpillar (*Manduca sexta*) midgut, where the ratio of columnar cells to goblet cells is approximately 2:1, no goblet cells were observed among the more than 3,000 cells that make up the midgut. How such a large pH gradient (luminal pH 11, cell pH 7) can be produced across the mosquito plasma membrane presents a challenge.

Do V-ATPases energize plasma membranes in all freshwater animals?

Wieczorek and Harvey (1995) have suggested that Na$^+$/K$^+$ P-ATPases are widely distributed on basolateral membranes of animal epithelia because that membrane faces the infamously constant 'internal environment' of Claude Bernard (1878/79), whereas H$^+$ V-ATPases are distributed in vacuoles of cells and apical (luminal) membranes of epithelia, because the 'external environment' is not constant. All freshwater animals live in an external environment that is Na$^+$-poor and osmotically hostile. H$^+$ V-ATPases are able to deal with this hostile environment by hyperpolarizing the apical membrane that drives Na$^+$ into the cells. Like *Aedes aegypti* larval midgut, crab (*Eriocheir sirensis*) gills (Onken and Putzenlechner, 1995) and clam (*Urio complaratus*) mantle (Hudson, 1993), the osmotically active membranes of virtually all freshwater animals may be energized by H$^+$ V-ATPases. The osmotically challenged membranes should then be sensitive to bafilomycin, immunolabeled with V-ATPase antibodies, studded with portasomes and hyperpolarized.

References

Anderson, E. and Harvey, W. R. (1966). Active transport by the Cecropia midgut. II. Fine structure of the midgut epithelium. *J. Cell Biol.* **31**, 107–134.

Azuma, M., Harvey, W. R. and Wieczorek, H. (1995). Stoichiometry of K+/H+ antiport helps to explain extracellular pH 11 in a model epithelium. *FEBS Lett.* **361**, 53–156.

Berenbaum, M. (1980). Adaptive significance of midgut pH in larval Lepidoptera. *Am. Nat.* **115**, 138–146.

Bernard, C. (1878/79). *Leçons sur les Phénomènes de la Vie Communs aux Animaux et aux Végétaux*. Baillere: Paris. In *Selected Readings in the History of Physiology* (translated by J. F. Fulton). Springfield, IL: Charles C. Thomas.

Bradley, T. J. and Satir, P. (1981). 5-Hydroxytryptamine-stimulated mitochondrial movement and microvillar growth in the lower Malpighian tubule of the insect, *Rhodnius prolixus. J. Cell Sci.* **49**, 139–161.

Brown, D. and Breton, S. (1996). Mitochondria-rich, proton-secreting epithelial cells. *J. Exp. Biol.* **199**, 2345–2358.

Brown, D., Sabolic, I. and Gluck, S. (1992). Polarized targeting of H+ V-ATPase in kidney epithelial cells. *J. Exp. Biol.* **172**, 231–243.

Brown, M. R., Raikhel, A. S. and Lea, A. O. (1985). Ultrastructure of midgut endocrine cells in the adult mosquito *Aedes aegypti. Tissue Cell* **17**, 709–721.

Castagna, M., Shayakul, C., Trotti, D., Sacchi, V. F., Harvey, W. R. and Hediger, M. A. (1998). Expression cloning and characterization of KAAT1, a potassium-coupled amino acid cotransporter. *Proc. Natl. Acad. Sci. USA* **95**, 5395–5400.

Cioffi, M. (1979). The morphology and fine structure of the larval midgut of a moth (*Manduca sexta*) in relation to active ion transport. *Tissue Cell* **11**, 467–479.

Cioffi, M. (1984). Comparative ultrastructure of arthropod transporting epithelia. *Am. Zool.* **24**, 139–156.

Cioffi, M. and Wolfersberger, M. G. (1983). Isolation of separate apical, lateral and basal plasma membrane from cells of an insect epithelium. A procedure based on tissue organization and ultrastructure. *Tissue Cell* **15**, 781–803.

Clark, T. M., Koch, A. and Moffett, D. F. (1999). The anterior and posterior 'stomach' regions of larval *Aedes aegypti* midgut: regional specialization of ion transport and stimulation by 5-hydroxytryptamine. *J. Exp. Biol.* **202**, 247–252.

Dadd, R. H. (1975). Alkalinity within the midgut of mosquito larvae with alkaline-active digestive enzymes. *J. Insect Physiol.* **21**, 1847–1853.

Dadd, R. H. (1976). Loss of midgut alkalinity in chilled or narcotized mosquito larvae. *Ann. Ent. Soc. Am.* **69**, 248–254.

Dow, J. A. T. (1984). Extremely high pH in biological systems: a model for carbonate transport. *Am. J. Physiol.* **246**, R633–R635.

Dow, J. A. T. and Peacock, J. M. (1989). Microelectrode evidence for the electric isolation of goblet cell cavities in *Manduca sexta* middle midgut. *J. Exp. Biol.* **143**, 101–114.

Dröse, S. and Altendorf, K. (1997). Bafilomycins and concanamycins as inhibitors of V-ATPases and P-ATPases. *J. Exp. Biol.* **200**, 1–8.

Garayoa, M., Villaro, A. C., Klein, U., Zimmermann, B., Montuenga, L. M. and Sesma, P. (1995). Immunocytochemical localization of a vacuolar-type ATPase in Malpighian tubules of the ant *Formica polyctena. Cell Tissue Res.* **282**, 343–350.

Gill, S. S., Chu, P. B., Smethurst, P., Pietrantonio, P. V. and Ross, L. S. (1998). Isolation of the V-ATPase A and c subunit cDNAs from mosquito midgut and Malpighian tubules. *Arch. Insect Biochem. Physiol.* **37**, 80–90.

Gräf, R., Harvey, W. R. and Wieczorek, H. (1996). Purification and properties of a cytosolic V1-ATPase. *J. Biol. Chem.* **271**, 20908–20913.

Gringorten, J. L., Crawford, D. N. and Harvey, W. R. (1993). High pH in the ectoperitrophic space of the larval lepidopteran midgut. *J. Exp. Biol.* **183**, 353–359.

Gupta, B. L. and Berridge, M. J. (1966). A coat of repeating subunits on the cytoplasmic surface of the plasma membrane in the rectal papillae of the blowfly, *Calliphora erythrocephala* (Meig.), studied *in situ* by electron microscopy. *J. Cell Biol.* **29**, 376–382.

Harvey, W. R. (1992). Physiology of V-ATPases. *J. Exp. Biol.* **172**, 1–17.

Harvey, W. R., Cioffi, M., Dow, J. A. T. and Wolfersberger, M. G. (1983). Potassium ion transport ATPase in insect epithelia. *J. Exp. Biol.* **106**, 91–117.

Harvey, W. R. and Wieczorek, H. (1997). Animal plasma membrane energization by chemiosmotic H+ V-ATPases. *J. Exp. Biol.* **200**, 203–216.

Hecker, H. (1977). Structure and function of midgut epithelial cells in *Culicidae* mosquitoes (Insect, Diptera). *Cell Tissue Res.* **184**, 321–341.

Hudson, R. L. (1993). Bafilomycin-sensitive acid secretion by mantle epithelium of the freshwater clam, *Unio complanatus. Am. J. Physiol.* **264**, R946–R951.

Jones, J. C. and Zeve, V. H. (1968). The fine structure of the gastric caeca of *Aedes aegypti. J. Insect Physiol.* **14**, 1567–1575.

Just, F. and Walz, B. (1994). Immunocytochemical localization of Na+/K+-ATPase and V-H+-ATPase in the salivary glands of the cockroach, *Periplaneta americana. Cell Tissue Res.* **278**, 161–170.

Klein, U., Timme, M., Zeiske, W. and Ehrenfeld, J. (1997). The H+ pump in frog skin (*Rana esculenta*): identification and localization of a V-ATPase. *J. Membr. Biol.* **157**, 117–126.

Linser, P. J., Schlosshauer, B., Galileo, D. S., Buzzi, W. R. and Lewis, R. (1997). Late proliferation of retinal Muller cell progenitors facilitates preferential targeting with retroviral vectors *in vitro. Dev. Genet.* **20**, 186–196.

Nelson, N. and Harvey, W. R. (1999). Vacuolar and plasma membrane V-ATPases. *Physiol. Rev.* **79** (in press).

Onken, H. and Putzenlechner, M. (1995). A V-ATPase drives active, electrogenic and Na+-independent Cl− absorption across the gills of *Eriocheir sinensis. J. Exp. Biol.* **198**, 767–774.

Radermacher, M., Ruis, T., Harvey, W. R., Wieczorek, H. and Grüber, G. (1999). Molecular architecture of *Manduca sexta* midgut V1ATPase visualized by electron microscopy. *FEBS Lett.* (in press).

Reynolds, E. S. (1963). The use of lead citrate at high pH as an electron opaque stain in electron microscopy. *J. Cell Biol.* **17**, 208–212.

Schirmanns, K. and Zeiske, W. (1994). An investigation of the midgut K+ pump of the tobacco hornworm (*Manduca sexta*) using specific inhibitors and amphotericin B. *J. Exp. Biol.* **188**, 191–204.

Schweikl, H., Klein, U., Schindlbeck, M. and Wieczorek, H. (1989). A vacuolar-type ATPase, partially purified from potassium transporting plasma membranes of tobacco hornworm midgut. *J. Biol. Chem.* **264**, 11136–111142.

Stevens, T. H. and Forgac, M. (1997). Structure, function and regulation of the vacuolar (H+)-ATPase. *Annu. Rev. Cell Dev. Biol.* **13**, 779–808.

Volkmann, A. and Peters, W. (1989a). Investigation on the midgut caeca of mosquito larva. I. Fine structure. *Tissue Cell* **21**, 243–251.

Volkmann, A. and Peters, W. (1989b). Investigation on the midgut caeca of mosquito larva.II. Functional aspects. *Tissue Cell* **21**, 253–261.

Wieczorek, H., Grüber, G., Harvey, W. R., Huss, M., and Merzendorfer, H. (1999). The plasma membrane H$^+$ V-ATPase from tobacco hornworm midgut. *J. Bioenerg. Biomembr.* **31**, 67–74.

Wieczorek, H., Cioffi, M., Klein, U., Harvey, W. R., Schweikl, H. and Wolfersberger, M. G. (1990). Isolation of goblet cell apical membrane from tobacco hornworm midgut and purification of its vacuolar-type ATPase. *Meth. Enzymol.* **192**, 608–616.

Wieczorek, H. and Harvey, W. R. (1995). Energization of animal plasma membranes by proton-motive force. *Physiol. Zool.* **68**, 15–23.

Wieczorek, H., Putzenlechner, M., Zeiske, W. M. and Klein, U. (1991). A vacuolar-type proton pump energizes K$^+$/H$^+$-antiport in an animal plasma membrane. *J. Biol. Chem.* **266**, 15340–15346.

Wieczorek, H., Weerth, S., Schindlbeck, M. and Klein, U. (1989). A vacuolar-type proton pump in a vesicle fraction enriched with potassium transporting plasma membrane from tobacco hornworm midgut. *J. Biol. Chem.* **264**, 11143–11148.

Wieczorek, H., Wolfersberger, M. G., Cioffi, M. and Harvey, W. R. (1986). Cation-stimulated ATPase activity in purified plasma membranes from tobacco hornworm midgut. *Biochim. Biophys. Acta* **857**, 271–281.

Wigglesworth, V. B. (1942). The storage of protein, fat, glycogen and uric acid in the fat body and other tissues of mosquito larvae. *J. Exp. Biol.* **19**, 56–77.